Roberts, A. L., "On the Melting of a Semi-Infinite Body Placed in a Warm Stream of Air," *J. Fluid Mech.*, 4, 505 (1958).
Savino, J. M., J. F. Zumdieck and R. Siegel, "Experimental Study of Freezing and Melting of Flowing Warm Water at a Stagnation Point on a Cold Plate," Fourth Int. Heat Transfer Conference, Paris-Versailles, 1, Cu 2.10 (1970).
Schlichting, H., *Boundary Layer Theory*, p. 83, McGraw-Hill, New York (1960).
Sitharamayya, S., and K. Subba Raju, "Heat Transfer Between an Axisymmetric Jet and a Plate Held Normal to the Flow," *Can. J. Chem. Eng.*, 47, 365 (1969).
Stewart, W. E., and R. Prober, "Heat Transfer and Diffusion in Wedge Flows with Rapid Mass Transfer," *Int. J. Heat Mass Transfer*, 5, 1149 (1962).
Swedish, M. J., M. Epstein, J. H. Linehan, G. A. Lambert, G. M. Hauser and L. J. Stachyra, "Surface Ablation in the Impingement Region of a Liquid Jet," *AIChE J.*, 25, 630 (1979).
Yang, K. T., "Formation of Ice in Plant Stagnation Flow," *Appl. Sci. Res.*, 17, 377 (1966).
Yim, A., M. Epstein, S. G. Bankoff, G. A. Lambert and G. M. Hauser, "Freezing-Melting Heat Transfer in a Tube Flow," *Int. J. Heat Mass Transfer*, 21, 1185 (1978).
Yen, Y. C., and A. Zehnder, "Melting Heat Transfer with Water Jet," *ibid.*, 16, 219 (1973).
Yen, Y. C., "Heat-Transfer Characteristics of a Bubble-Induced Water Jet Impinging on an Ice Surface," *ibid.*, 18, 917 (1975).

Manuscript received March 12, 1979; revision received February 12, and accepted February 29, 1980.

Viscous Heat Generation in Slit Flow

The onset of significant departure from isothermality caused by viscous energy dissipation in flow through a slit is determined for isothermal and adiabatic walls. A series solution of the energy equation enables calculation of dimensionless profiles for any power law fluid. Such solutions provide useful standards for judging performances of numerical schemes for solving complex nonisothermal flows.

ROBERT M. YBARRA
and
ROGER E. ECKERT
School of Chemical Engineering
Purdue University
West Lafayette, Indiana 47907

SCOPE

When a viscous fluid in a slit is set in flow by a large imposed pressure gradient, a vast amount of mechanical energy is converted irreversibly into heat owing to the fluid's internal friction. This viscous heat dissipation not only leads to an overall increase in the fluid's bulk temperature but also causes a noticeable temperature variation to develop across the shear field. Significant viscous heating occurs when the heat generated by the shearing of adjacent fluid layers is on the order of the heat which is removed by conduction through a slit wall. Since rheological properties, such as viscosity, are strongly temperature dependent, any rheological measurement not conducted under completely isothermal conditions can be erroneous and the observed fluid behavior misleading. In fact, heat effects can induce an apparent non-Newtonian behavior in Newtonian fluids.

The apparent nonlinear behavior which is exhibited by a general fluid undergoing deformation may be the result of two different mechanisms. The first is the dependence of the rheological properties on the fluid's state of deformation. This mechanism has been the major concern of most of the research in non-Newtonian fluid mechanics. The second mechanism is the dependence of the rheological properties on the thermodynamic state of the fluid, that is, the temperature and pressure. Since most fluids are relatively incompressible, except at extremely high pressures, the effect of pressure on the rheological behavior is neglected in this work. Variation in temperature due to shearing and resultant heat transfer in flow through a slit is treated.

The parallel plate geometry plays a significant part in such polymer processing operations as extrusion of thin film and flow of molten polymer through the shallow channel of a screw pump. Furthermore, experimental investigations (Novotny and Eckert, 1973, 1974) have clearly established that the slit geometry is an advantageous means of accurately determining rheological properties of viscoelastic liquids in the high shear flow regime, a region where most macromolecular fluids are processed. However, the use of the slit as a rheological geometry is not widespread. Moreover, the study of the nonisothermal slit flow of non-Newtonian fluids has received relatively little attention despite the industrial and scientific importance of this geometry.

Laminar heat transfer of a non-Newtonian fluid in slit flow but without viscous heat generation has been dealt with by several authors (Tien, 1962; Suckow et al., 1971; Kwant and Van Ravenstein, 1973). The first two authors developed solutions to the slit's analogue of the Graetz-Nusselt problem for power law fluids, whereas Kwant and Van Ravenstein studied the heat transfer rate and the effect of this transfer upon the hydrodynamics for power law fluids.

At the high shear rates normally used to process macromolecular fluids in parallel plate channels, considerable heat is generated, but this topic has been treated by relatively few investigators. Seifert (1969) calculated the developing temperature profile for a Prandtl-Eyring fluid with emphasis on the heat flux at the slit wall for symmetric and asymmetric wall temperatures. Vlachopoulos and Keung (1972) numerically solved the energy equation for a power law fluid in fully developed flow and presented the results in terms of the Nusselt number and bulk temperature rise. Cox and Macosko (1974) experimentally investigated the surface temperature rise of poly(acrylonitrile cobutadiene-styrene) (ABS) and polyethylene (PE) extruded through slits and associated geometries using an infrared pyrometer. For fluids with variable density and shear and temperature dependent viscosity, they numerically treat the mass, momentum and energy equations. Winter (1975, 1977) treated the viscous dissipation problem for a power law fluid whose viscosity decreases exponentially with temperature using an implicit iterative numerical scheme for the solution of the equations of change.

In the present work, analytical solutions are obtained for the problem of viscous generation for non-Newtonian fluids in slit flow. Both isothermal and adiabatic slit wall cases are treated. The fluids studied are assumed to be adequately described by a power law shear stress dependence. Since our ultimate goal is

to determine when viscous dissipation significantly influences the fluid temperature and thus property determination, it is sufficient to use temperature independent properties. It is this simplification that enables us to obtain an analytical solution in contrast to the above numerical solutions.

The solution is analogous to the Graetz type of series expansion of the viscous heating problem in a capillary considered by Brinkman (1951) (Newtonian fluid) and Bird (1955) (power law fluid). However, we have opted to solve for the eigenvalues and eigenfunctions numerically by a finite difference scheme rather than the power series expansion technique employed by Brinkman and Bird. In this manner we can solve the problem for any value of the continuous exponent n in the power law. In contrast, solution by the power series expansion is very limited, since the derivatives of the approximating series must be continuous, and this only occurs when n is a reciprocal of an integer. This restriction is extremely limiting because few non-Newtonian fluids have n values of exactly one-half, one-third, one-fourth, etc. In addition, the technique we employ in the solution of the energy equation can be generally useful in the numerical treatment of certain linear characteristic value problems.

CONCLUSION AND SIGNIFICANCE

The energy equation is solved for incompressible viscous flow through a long slit. An accurate series solution for the temperature profile is obtained by the numerical determination of the eigenvalues and eigenfunctions via a finite difference scheme. The reduced temperature profiles and corresponding maximum and bulk temperature rises are presented as functions of the dimensionless axial distance. Isothermal and insulated wall cases are treated for the range of exponents of the power law model commonly encountered in polymeric liquids. The method used to evaluate the eigenvalue problems allows any power law fluid, either pseudoplastic or dilatant in behavior, to be treated; graphs of the solution are presented for n of 0.25, 0.35, 0.50, 0.75 and 1.0 (Figures 3 to 12) and can be conveniently interpolated.

The dimensionless form in which our solution is expressed also enables us to determine how the slit geometry can be varied to reduce the effect of viscous heating. A detailed analysis shows how to design slits to minimize the effect of viscous heating during property determination. For any shear rate, the slit thickness is the variable found to have the greatest influence upon the extent of temperature rise; thin slits are the best design to minimize the effect of viscous shear.

Our study enables the investigation of generated thermal effects which can adversely affect the determination of rheological properties of viscous liquids in a slit rheometer. Since the viscosity for most viscous Newtonian and polymeric liquids decreases several percent per centigrade degree rise, rheological properties are suspect when the departure from isothermality due to viscous shear reaches a few centigrade degrees. We provide an example which demonstrates the application of our solution for calculating the extent of viscous heating in a slit. Also, industrial processing of viscous fluids is usually conducted at high shear rates for optimum productivity. The considerable energy dissipated during flow raises the fluid temperature. Therefore, an additional use of our study is to allow the design engineer to determine when a sizable temperature rise will result in such industrial operations as the extrusion of films or thin walled tubing and lubrication in narrow slits and annuli. Under conditions where viscous heating is appreciable, flow design calculations based upon an isothermal assumption are of questionable value.

With many numerical schemes being developed to take into account such complexities as temperatures dependent properties (for example, Winter, 1977), it is important to have exact solutions as base cases to evaluate the accuracy of such procedures. We have verified the accuracy of our solution technique against an extremely accurate solution for a simpler but related eigenvalue problem. The results of our study, therefore, provide a useful test for assessing future as well as existing numerical programs.

FORMULATION OF THE PROBLEM

We shall consider steady nonisothermal flow of an incompressible fluid in a long slit in which all explicit time derivatives are zero. Furthermore, we shall treat the problem where the Reynolds number is small or moderate but the Prandtl number is large. Under these conditions, the flow field in the slit will be laminar and will develop in a much shorter distance than does the temperature field. Therefore, the velocity field can be approximated as fully developed at the slit entrance. These constraints on the Reynolds and Prandtl numbers are realistic for the physical situation of polymer processing, where typical estimates are $N_{Re} \simeq 10^{-3}$ and $N_{Pr} \simeq 10^{6}$. The Peclet number N_{Pe} is, therefore, on the order of 10^{3} which permits the heat transfer by conduction in the flow direction x_1 to be neglected. Prior to solving nonisothermal flow problems with temperature dependent viscosities, the viscosity must be measured under several isothermal conditions. Our emphasis is prediction of conditions which cause sufficient heat generation to vitiate rheological property determination. For this purpose, the fluid properties can be taken to be independent of temperature. In addition, the normal stresses, which are present in the slit flow of polymeric liquids, are assumed to exhibit a negligible effect upon the temperature distribution.

For the flow geometry shown in Figure 1 with the assumptions described above, the temperature distribution in a slit involves the solution of the following two uncoupled linear partial differential equations:

$$\frac{\partial p}{\partial x_1} + \frac{\partial \tau_{12}}{\partial x_2} = 0 \tag{1}$$

$$\rho \hat{C}_p v_1 \frac{\partial T}{\partial x_1} = k \frac{\partial^2 T}{\partial x_2^2} + \tau_{12} \frac{\partial v_1}{\partial x_2} \tag{2}$$

As can be seen from the above set of equations, a rheological equation of state is required for their solution. Since the heat generation in shear flow has been assumed to be a purely viscous effect, then any generalized Newtonian fluid model should adequately serve as an appropriate choice:

$$\tau_{12} = \eta(\dot{\gamma})\,\dot{\gamma} \tag{3}$$

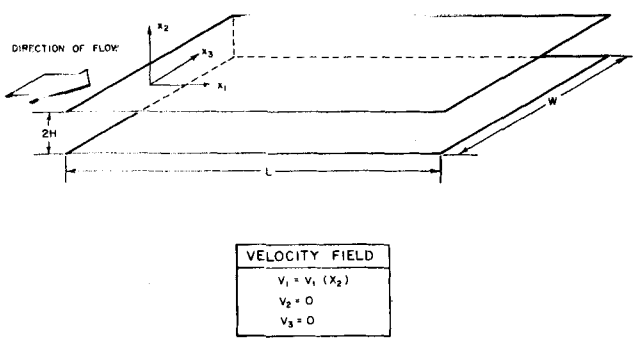

Figure 1. Flow geometry in the slit channel.

The particular generalized Newtonian model we have selected to treat is the power law model

$$\eta = K\dot{\gamma}^{n-1} \tag{4}$$

For shear flow in a slit, Equation (3) becomes

$$\tau_{12} = K\left(-\frac{\partial v_1}{\partial x_2}\right)^{n-1}\frac{\partial v_1}{\partial x_2} \tag{5}$$

The selection of the power law model in our study is based upon the fact that a majority of the literature on the viscous heating of non-Newtonian fluids in other rheometers uses the power law or modified power law model. The types of viscometric flow situations which have been studied are as follows: capillary (Bird, 1955; Gee and Lyon, 1956; Toor 1956, 1957; Sukanek, 1971; Cox and Macosko, 1974; Galili et al., 1975*a*, 1975*b*; Winter, 1975; Hieber, 1977; Dang, 1979), cone and plate (Turian, 1965), Couette (Bird et al., 1960; Tien, 1961; Middleman, 1968; Gavis and Laurence, 1968).

Upon substituting Equation (5) into Equation (1) and (2), we find

$$-\frac{\partial p}{\partial x_1} + K\frac{\partial}{\partial x_2}\left[\left(-\frac{\partial v_1}{\partial x_2}\right)^n\right] = 0 \tag{6}$$

$$\rho\hat{C}_p v_1\left(\frac{\partial T}{\partial x_1}\right) = k\frac{\partial^2 T}{\partial x_2^2} + K\left(-\frac{\partial v_1}{\partial x_2}\right)^{n+1} \tag{7}$$

The two problems that we wish to solve are the isothermal wall, where the fluid enters the slit at the same temperature as the wall, and the adiabatic wall, where the net flux of energy through the wall is zero. These two boundary conditions which we shall impose on the slit's walls represent the extremes of all real heat transfer situations, ones of mixed boundary conditions. Most of the previous treatments on the nonisothermal flow in slits have imposed a slightly different isothermal wall situation than ours, that is, one which has the fluid entering at a temperature which is different than the wall temperature. We shall discuss later how our solution can be modified to also handle this case. As for the adiabatic wall case, a table in Winter's review paper (1977) on the studies of viscous heating in shear flow shows that no solution, either analytical or numerical, exists for flow through insulated slit dies.

We have defined for study the case with the wall temperature the same as the initial fluid temperature as isothermal wall. Rheological measurements should be conducted in this manner, as any heating or cooling of the fluid introduced by subjecting the slit walls to a temperature different than the entering fluid would certainly vitiate the determined properties.

The fluid is assumed to have zero slip at the wall; therefore, the applicable boundary conditions on the velocity profile are

$$\begin{aligned} \frac{\partial v_1}{\partial x_2} &= 0 \quad \text{at} \quad x_2 = 0, \quad 0 < x_1 < L \\ v_1 &= 0 \quad \text{at} \quad x_2 = H, \quad 0 < x_1 < L \end{aligned} \tag{8}$$

The necessary boundary conditions for the temperature distribution in the isothermal wall problem are

$$\begin{aligned} \frac{\partial T}{\partial x_2} &= 0 \quad \text{at } x_2 = 0, \quad 0 < x_1 < L \\ T &= T_w \quad \text{at } x_2 = H \quad 0 < x_1 < L \\ T &= T_w \quad \text{at } x_1 = 0, \quad 0 < x_2 < H \end{aligned} \tag{9}$$

For the adiabatic wall problem, the boundary conditions are

$$\begin{aligned} \frac{\partial T}{\partial x_2} &= 0 \quad \text{at } x_2 = 0, \quad 0 < x_1 < L \\ \frac{\partial T}{\partial x_2} &= 0 \quad \text{at } x_2 = H, \quad 0 < x_1 < L \\ T &= T_0 \quad \text{at } x_1 = 0, \quad 0 < x_2 < H \end{aligned} \tag{10}$$

Since Equations (6) and (7) are uncoupled, we can solve for the velocity profile separate from the temperature distribution. The solution to the velocity distribution has been presented elsewhere (Wohl, 1968), and the results are

$$v_1 = V_{\max}\left[1 - \left(\frac{x_2}{H}\right)^N\right] \tag{11}$$

where

$$V_{\max} = \left[\frac{1}{K}\left(-\frac{\partial p}{\partial x_1}\right)H\right]^{1/n}\frac{H}{N} = \left[\frac{\tau_w}{K}\right]^{1/n}\frac{H}{N} \tag{12}$$

and $N = (n + 1)/n$.

It is convenient to rewrite Equation (7) in dimensionless form by introducing the following dimensionless variables:

reduced transverse distance:

$$\eta = \frac{x_2}{H} \tag{13}$$

reduced axial distance:

$$\psi = \frac{kx_1}{\rho\hat{C}_p H^2 V_{\max}} = \left(\frac{x_1}{H}\right)N_{Pe}^{-1} \tag{14}$$

reduced temperature rise:

$$\theta = \frac{T - T_w}{T_w} \quad \text{(isothermal wall)} \tag{15}$$

$$\theta = \frac{T - T_0}{T_0} \quad \text{(adiabatic wall)} \tag{16}$$

In Equations (15) and (16), absolute temperatures are used in the denominators which represent a temperature difference above absolute zero. Therefore, the equations are truly dimensionless, with units of temperature difference in both numerator and denominator. The form selected leads to homogeneous boundary conditions.

Thus, the mathematical problem to be solved is

$$(1 - \eta^N)\frac{\partial\theta}{\partial\psi} = \frac{\partial^2\theta}{\partial\eta^2} + N_{Br}\,\eta^N \tag{17}$$

with the boundary conditions

isothermal wall:

$$\begin{aligned} \frac{\partial\theta}{\partial\eta} &= 0 \quad \text{at } \eta = 0 \\ \theta &= 0 \quad \text{at } \eta = 1 \\ \theta &= 0 \quad \text{at } \psi = 0 \end{aligned} \tag{18}$$

adiabatic wall:

$$\begin{aligned} \frac{\partial\theta}{\partial\eta} &= 0 \quad \text{at } \eta = 0 \\ \frac{\partial\theta}{\partial\eta} &= 0 \quad \text{at } \eta = 1 \\ \theta &= 0 \quad \text{at } \psi = 0 \end{aligned} \tag{19}$$

The quantity N_{Br} is the Brinkman number for a power law fluid and is defined as

$$N_{Br} = \frac{K H^2\left[N\left(\frac{V_{\max}}{H}\right)\right]^{n+1}}{kT_w} \tag{20}$$

The above expression of the Brinkman number is for the isothermal wall problem. If we were to consider the isothermal wall problem where the wall temperature T_w differs from the fluid's initial temperature T_0, then the quantity $T_0 - T_w$ would replace T_w in the denominator of Equations (15) and (20), and the condition of $\psi = 0$ would become $\theta = 1$. For the adiabatic wall case, we replace T_w by T_0 in Equation (20) to obtain the

Brinkman number. Since the Brinkman number is the ratio of heat generated by viscous dissipation to the heat transferred via conduction through the fluid media, then its magnitude in Equation (17) will provide us with a measure of the extent to which viscous heating alters the fluid temperature.

SOLUTION TO THE DIFFERENTIAL EQUATION FOR THE TEMPERATURE DISTRIBUTION

For both the isothermal wall and adiabatic wall problems, the well-known technique of the separation of variables (Churchill, 1963) can be employed if the linear partial differential Equation (17) as well as its respective boundary conditions can be rendered homogeneous. We shall appeal to our physical intuition of the problem in order to afford transformations of variables which accomplish our aim.

Isothermal Wall

In the case of the isothermal wall, we know that for large distances down the slit, a temperature distribution should be attained which depends solely on the transverse distance. Therefore, it would be reasonable to propose the following transformation:

$$\theta(\eta,\psi) = \Xi(\eta,\psi) + \phi(\eta) \tag{21}$$

The solution to $\phi(\eta)$ is a straightforward integration which yields

$$\phi(\eta) = \frac{N_{Br}}{(N+1)(N+2)}(1 - \eta^{N+2}) \tag{22}$$

The solution of the homogeneous partial equation in $\Xi(\eta,\psi)$ will be given in the next section. The function $\phi(\eta)$ represents the fully developed temperature distribution.

Adiabatic Wall

In flow through a slit with its wall operating adiabatically, a steady temperature distribution is never realized. The fact that the slit is adiabatic causes the temperature to increase with distance downstream. At a considerable distance downstream, the form of the transverse temperature dependence will become fixed. Further increase in temperature will be due only to the axial distance. Thus, we shall introduce the transformation

$$\theta(\eta,\psi) = \Xi(\eta,\psi) + \phi(\eta) + \chi(\psi) \tag{23}$$

This transformation results in a separable differential equation in $\phi(\eta)$ and $\chi(\psi)$. Integration of the two ordinary differential equations gives

$$\chi(\psi) = \frac{N_{Br}}{N}\psi \tag{24}$$

$$\phi(\eta) = \frac{N_{Br}}{2N}\left[\eta^2 - \frac{2}{(N+2)}\eta^{N+2}\right] \tag{25}$$

The solution of the differential equation in $\Xi(\eta,\psi)$ is provided later. The addition of Equations (24) and (25) represents the temperature distribution for very large ψ. We see that the temperature distribution at very large ψ varies linearly with ψ about an established profile in η.

GENERAL SOLUTION TO HOMOGENEOUS DIFFERENTIAL EQUATION

When the expression for the temperature distribution at very large ψ is substituted into Equation (17), the following differential equation of Ξ is obtained for both the isothermal and adiabatic wall problems:

$$(1 - \eta^N)\frac{\partial \Xi}{\partial \psi} = \frac{\partial^2 \Xi}{\partial \eta^2} \tag{26}$$

The solutions for Ξ are different for isothermal and adiabatic wall problems owing to the fact that their respective boundary conditions are dissimilar.

By the classical technique of separation of variables, we postulate the solution to Equation (26) of the form $\Xi(\eta,\psi) = F(\eta)G(\psi)$ which reduces the partial differential Equation (26) to two ordinary differential equations

$$F''(\eta) + \lambda(1 - \eta^N)F(\eta) = 0 \tag{27}$$

$$G'(\psi) + \lambda G(\psi) = 0 \tag{28}$$

subject to the appropriate boundary conditions. The solution to the boundary value problem (27) has an infinite set of solutions $F_n(\eta)$ corresponding to an infinite set of eigenvalues λ_n. Its solution, which we determined numerically by a finite difference, will be described later. Equation (28) has a facile solution. The expression for $\Xi(\eta,\psi)$ by the superposition principle must be given by products of functions of η and ψ because of the linearity of the original partial differential Equation (26). When this solution is combined with the results of the previous section, the final expressions for the temperature distribution θ have the form

isothermal wall:

$$\theta = \frac{N_{Br}}{(N+1)(N+2)}\left[(1 - \eta^{N+2}) + \sum_{n=1}^{\infty} C_n F_n(\eta)\exp(-\lambda_n\psi)\right] \tag{29}$$

adiabatic wall:

$$\theta = \frac{N_{Br}}{2N}\left[\eta^2 - \frac{2}{(N+2)}\eta^{N+2} + 2\psi + \sum_{n=1}^{\infty} C_n F_n(\eta)\exp(-\lambda_n\psi)\right] \tag{30}$$

The constants C_n which appear in Equations (29) and (30) are determined by applying the boundary conditions at $\psi = 0$, by multiplying the result by $F_m(\eta)(1 - \eta^N)d\eta$ and by integrating from $\eta = 0$ to $\eta = 1$. In this manner, the two expressions for constants are obtained:

isothermal wall:

$$C_n = -\frac{\int_0^1 [1 - \eta^{N+2}][1 - \eta^N] F_n(\eta)\, d\eta}{\int_0^1 [1 - \eta^N] F_n^2(\eta)\, d\eta} \tag{31}$$

adiabatic wall:

$$C_n = -\frac{\int_0^1 \left[\eta^2 - \frac{2}{(N+2)}\eta^{N+2}\right]\left[1 - \eta^N\right] F_n(\eta)\, d\eta}{\int_0^1 [1 - \eta^N] F_n^2(\eta)\, d\eta} \tag{32}$$

The above expressions were evaluated by numerical integration. The results will be presented later. If we want the solution to the isothermal wall problem where the fluid enters at a temperature different from the wall, Equation (29) will still apply, and a new set of C_n's must be calculated owing to the different boundary condition subjected at $\psi = 0$. This calculation can be handled by a simple replacement of $(1 - \eta^{N+2}) - (N + 1)(N + 2)/N_{Br}$ for $1 - \eta^{N+2}$ in Equation (31). However, the fact that the Brinkman cannot be factored out of the integral requires a new set of C_n's to be evaluated for each Brinkman number of interest.

AVERAGE TEMPERATURE RISE

With the temperature distribution known from Equations (29) and (30), it is now possible to calculate the average temperature rise in the slit. We are particularly interested in the bulk or mixing-cup temperature, since it can be easily measured at the

$$\underline{\underline{A}}\,\underline{f} = \lambda \underline{\underline{B}}\,\underline{f} \qquad (5\text{-}47)$$

$$\begin{vmatrix} F_1 - 2F_2 & & & & \\ F_1 - 2F_2 & F_3 & & & \\ & F_2 - 2F_3 & F_4 & & \\ & & \cdots\cdots & & \\ & & F_{M-2} - 2F_{M-1} & F_M & \\ & & F_{M-1} - 2F_M & & \end{vmatrix} = h^2 \begin{vmatrix} \frac{1}{2}F_1 & & & & \\ -\frac{3}{40}F_1 & -\frac{209}{240}r_2F_2 & -\frac{1}{60}r_3F_3 & -\frac{7}{120}r_4F_4 & \frac{1}{40}r_5F_5 & -\frac{1}{240}r_6F_6 \\ \frac{1}{240}F_1 & -\frac{1}{10}r_2F_2 & -\frac{97}{120}r_3F_3 & -\frac{1}{10}r_4F_4 & \frac{1}{240}r_5F_5 & \\ & & \cdots\cdots & & & \\ & & \frac{1}{240}r_{M-3}F_{M-3} & -\frac{1}{10}r_{M-2}F_{M-2} & -\frac{97}{120}r_{M-1}F_{M-1} & -\frac{1}{10}r_MF_M \\ & -\frac{1}{240}r_{M-4}F_{M-4} & -\frac{1}{40}r_{M-3}F_{M-3} & -\frac{7}{120}r_{M-2}F_{M-2} & -\frac{1}{60}r_{M-1}F_{M-1} & -\frac{209}{240}r_MF_M \end{vmatrix}$$

Figure 2. For the isothermal wall case, this matrix equation is solved for the eigenvalues and eigenfunctions, Equation (47).

exit. The mixing-cup temperature for a slit is defined by

$$\theta_{av} = \frac{\int_0^1 v_1(\eta)\ \theta(\eta,\psi)d\eta}{\int_0^1 v_1(\eta)d\eta} \qquad (33)$$

Substituting the velocity profile into Equation (33), we obtain

$$\theta_{av} = \frac{N+1}{N}\int_0^1 (1-\eta^N)\theta(\eta,\psi)d\eta \qquad (34)$$

This expression is valid for the isothermal and adiabatic wall problems when the proper temperature distribution is used.

METHOD OF THE NUMERICAL SOLUTION TO THE EIGENVALUE PROBLEM

The problem we are addressing is the solution of the equation

$$F''(\eta) + \lambda(1-\eta^N)F(\eta) = 0 \qquad (35)$$

subject to the boundary conditions for the isothermal wall

$$\begin{aligned} F'(0) &= 0 \\ F(1) &= 0 \end{aligned} \qquad (36)$$

and for the adiabatic wall

$$\begin{aligned} F'(0) &= 0 \\ F'(1) &= 0 \end{aligned} \qquad (37)$$

Equation (35) is a linear second-order differential equation of the form

$$y'' + f(x)y = 0 \qquad (38)$$

which can be solved by approximating the differential equation with a difference equation and subsequently satisfying a simultaneous set of algebraic equations at equally spaced points (Hildebrand, 1974).

We divide the differential equation in M equal intervals, thus creating $M+1$ points at which we generate a solution to the equation. The grid points F_1 and F_{M+1} represent the boundary points at the center line of the slit and wall, respectively. We chose to approximate the differential equation at the interior grid points $m = 2,3,\ldots,M$ with a seventh-order procedure in the sense that it would afford exact results if $F(\eta)$ were a polynomial of degree 7 or less. The boundary conditions are evaluated by a forward difference at the center line ($\eta = 0$) and a backward difference at the wall.

The results of the finite differencing Equation (35) are given below:

center boundary point ($m = 1$)

$$F_1\left[1 - \frac{h^2}{2}\lambda\right] - F_2 = 0 \qquad (39)$$

This condition applies for both isothermal and adiabatic wall problems. Error of this approximation is fourth order in the step size $h = 1/M$.

wall boundary point ($m = M+1$)

isothermal wall

$$F_{M+1} = 0 \qquad (40)$$

adiabatic wall

$$F_{M+1}\left\{1 + \left[\frac{h^3}{6} - (N-1)\frac{h^4}{24}\right]N\lambda\right\} - F_M = 0 \qquad (41)$$

The error in the boundary condition at the wall for the adiabatic wall is fifth order in h.

general interior points ($m = 2,3,\ldots,M$)

isothermal wall

For $m = 2$

$$\frac{3h^2}{40}\lambda F_1 - 2\left[1 - \frac{209h^2}{480}\lambda r_2(\eta)\right]F_2 + \left[1 + \frac{h^2}{60}\lambda r_3(\eta)\right]F_3 + \frac{7h^2}{120}\lambda r_4(\eta)F_4 - \frac{h^2}{40}\lambda r_5(\eta)F_5 + \frac{h^2}{240}\lambda r_6(\eta)F_6 = 0 \qquad (42)$$

For $m = 3,4,\ldots,M-2$

$$-\frac{h^2}{240}\lambda r_{m-2}(\eta)F_{m-2} + \left[1 + \frac{h^2}{10}\lambda r_{m-1}(\eta)\right]F_m - 2\left[1 - \frac{97h^2}{240}\lambda r_m(\eta)\right]F_m + \left[1 + \frac{h^2}{10}\lambda r_{m+1}(\eta)\right]F_{m+1} - \frac{h^2}{240}\lambda r_{m+2}(\eta)F_{m+2} = 0 \qquad (43)$$

For $m = M-1$

$$-\frac{h^2}{240}\lambda r_{M-3}(\eta)F_{M-3} + \left[1 + \frac{h^2}{10}\lambda r_{M-2}(\eta)\right]F_{M-2} - 2\left[1 - \frac{97h^2}{240}\lambda r_{M-1}(\eta)\right]F_{M-1} + \left[1 + \frac{h^2}{10}\lambda r_M(\eta)\right]F_M = 0 \qquad (44)$$

For $m = M$

$$\frac{h^2}{240}\lambda r_{M-4}(\eta)\,F_{M-4} + \frac{h^2}{40}\lambda r_{M-3}(\eta)\,F_{M-3} + \frac{7h^2}{120}\lambda r_{M-2}(\eta)\,F_{M-2} + \left[1 + \frac{h^2}{60}\lambda r_{M-1}(\eta)\right]F_{M-1} - 2\left[1 - \frac{209h^2}{480}\lambda r_M(\eta)\right]F_M = 0 \qquad (45)$$

where

$$r_m(\eta) = 1-\eta^N = 1 - [(m-1)h]^N$$

adiabatic wall

For $m = 2$ and $m = 3,4,\ldots,M-1$, the differential equation is approximated by Equations (42) and (43), respectively.

For $m = M$

$$\frac{h^2}{240}\lambda r_{M-4}(\eta)\,F_{M-4} - \frac{h^2}{40}\lambda r_{M-3}(\eta)\,F_{M-3} + \frac{7h^2}{120}\lambda r_{M-2}(\eta)\,F_{M-2} + \left[1 + \frac{h^2}{60}\lambda r_{M-1}(\eta)\right]F_{M-1} - 2\left[1 - \frac{209h^2}{480}\lambda r_M(\eta)\right]F_M + F_{M+1} = 0 \qquad (46)$$

The above equations generate the necessary system of equations in the unknown functions F_m and the unknown characteristic values λ_m. For example, the system of equations for the isothermal wall case is shown in Figure 2, where F_n is the eigenvector which corresponds to the n^{th} eigenvalue. Equation (47) is a general eigenvalue problem which can be solved by such computer programs as RGGEIG in the EISPACK package available from the Argonne National Laboratory. In this study, we have taken $M = 100$, which results in the highly accurate values shown later.

TABLE 1. CONSTANTS FOR USE IN EQUATIONS (29) AND (30) WHEN $n = 1.0$

	Isothermal wall		Adiabatic wall	
i	λ_i	C_i	λ_i	C_i
1	2.82776	1.1498	0.0000	0.1571
2	32.1472	−0.1909	18.3853	−0.1841
3	93.4740	0.0582	68.9743	0.0363
4	186.801	−0.0261	151.606	−0.0138
5	312.126	0.0142	266.266	0.0069
6	469.444	−0.0088	412.949	−0.0041

TABLE 2. CONSTANTS FOR USE IN EQUATIONS (29) AND (30) WHEN $n = 0.5$

	Isothermal wall		Adiabatic wall	
i	λ_i	C_i	λ_i	C_i
1	2.6459	1.1772	0.0000	0.1926
2	28.1319	−0.2336	15.8336	−0.2288
3	81.566	0.0803	59.8425	0.0488
4	162.898	−0.0367	131.811	−0.0184
5	272.117	0.0203	231.709	0.0093
6	409.222	−0.0127	359.525	−0.0055

RESULTS

In this section, we present the results of the numerical solution of Equation (35) subject to the prescribed boundary conditions Equations (36) and (37) for a Newtonian fluid and power law fluids with $n = 0.25$, 0.35, 0.50 and 0.75. The first six eigenvalues for the Newtonian fluid are presented in Table 1 and for the power law fluid with $n = 0.50$ in Table 2. The coefficients

TABLE 3. EIGENFUNCTIONS $F_n(\eta)$ FOR USE IN EQUATIONS (29) AND (30) WHEN $n = 1.0$

	Isothermal wall					Adiabatic wall			
η	F_1	F_2	F_3	F_4	F_5	F_2	F_3	F_4	F_5
0.0	1.00000	1.00000	1.00000	1.00000	1.00000	1.00000	1.00000	1.00000	1.00000
0.1	0.98592	0.84377	0.56851	0.20347	−0.19387	0.90962	0.67497	0.33381	−0.06008
0.2	0.94434	0.42615	−0.35128	−0.92130	−0.94134	0.65633	−0.08598	−0.77823	−1.00477
0.3	0.87722	−0.12048	−0.98431	−0.63420	0.50162	0.28870	−0.79669	−0.89673	0.11622
0.4	0.78760	−0.63451	−0.84139	0.60163	0.86311	−0.12720	−1.03716	0.09186	1.04125
0.5	0.67930	−0.98322	−0.07496	1.03500	−0.61220	−0.52476	−0.70572	0.99650	0.04071
0.6	0.55600	−1.10135	0.75398	0.17430	−0.97127	−0.85206	−0.01928	0.88387	−1.08326
0.7	0.42380	−0.99732	1.16688	−0.91422	0.34097	−1.08136	0.68523	−0.03463	−0.63088
0.8	0.28480	−0.73109	1.04990	−1.23289	1.27081	−1.21114	1.16607	−0.96254	0.64393
0.9	0.14285	−0.37873	0.58311	−0.76562	0.92848	−1.26199	1.37076	−1.41888	1.42798
1.0	0.00000	0.00000	0.00000	0.00000	0.00000	−1.26941	1.40140	−1.49012	1.55784

Note: F_1 for the adiabatic wall problem is 1.000 for all values of η.

TABLE 4. EIGENFUNCTIONS $F_n(\eta)$ FOR USE IN EQUATIONS (29) AND (30) WHEN $n = 0.5$

	Isothermal wall					Adiabatic wall			
η	F_1	F_2	F_3	F_4	F_5	F_2	F_3	F_4	F_5
0.0	1.00000	1.00000	1.00000	1.00000	1.00000	1.00000	1.00000	1.00000	1.00000
0.1	0.98680	0.86262	0.61915	0.29021	−0.07885	0.92188	0.71543	0.41022	0.04849
0.2	0.94758	0.48850	−0.23296	−0.83198	−0.98967	0.69990	0.02405	−0.66350	−0.99675
0.3	0.88355	−0.01893	−0.91047	−0.78423	0.22144	0.36944	−0.68180	−0.96283	−0.15928
0.4	0.79685	−0.52197	−0.91419	0.35449	0.98025	−0.01738	−1.01155	−0.15344	0.98691
0.5	0.69047	−0.89183	−0.26221	1.03208	−0.27499	−0.40217	−0.80201	0.83674	0.36076
0.6	0.56814	−1.04817	0.57361	0.40855	−1.03789	−0.73275	−0.18836	0.96312	−0.91248
0.7	0.43402	−0.97859	1.07318	−0.71036	0.05255	−0.97447	0.51734	0.17116	−0.79523
0.8	0.29232	−0.73070	1.03006	−1.17106	1.14577	−1.11696	1.03639	−0.78820	0.42605
0.9	0.14676	−0.38168	0.58647	−0.76702	0.92502	−1.17489	1.26952	−1.30249	1.29516
1.0	0.00000	0.00000	0.00000	0.00000	0.00000	−1.18360	1.30576	−1.38655	1.44808

Note: F_1 for the adiabatic wall problem is 1.000 for all values of η.

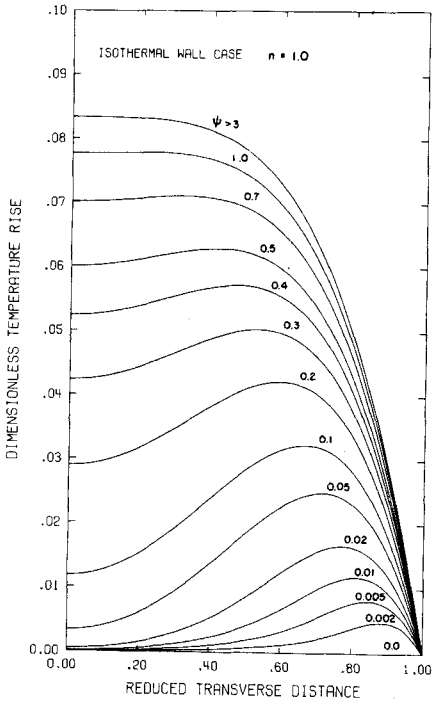

Figure 3. Dimensionless temperature profiles for a Newtonian fluid flowing in a slit whose walls are maintained at a constant temperature ($N_{Br}=1$).

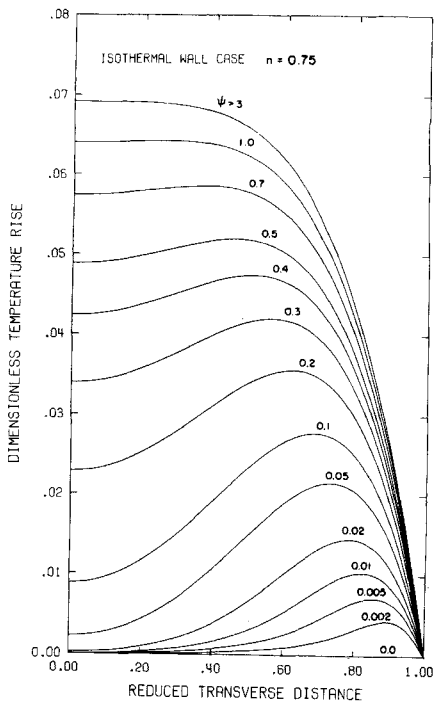

Figure 4. Dimensionless temperature profiles for a power law fluid with $n=0.75$ flowing in a slit whose walls are maintained at a constant temperature ($N_{Br}=1$).

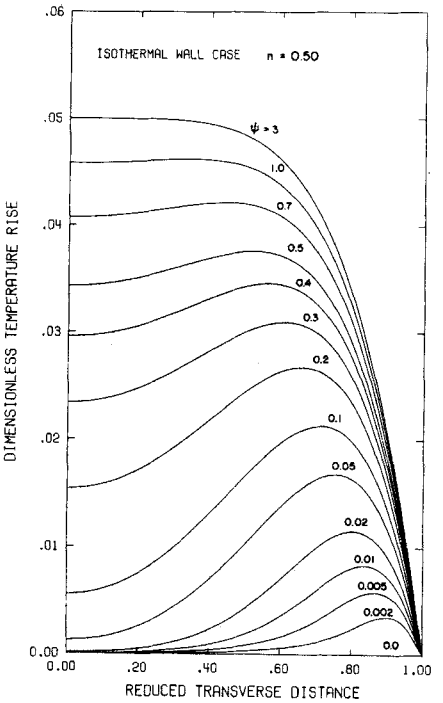

Figure 5. Dimensionless temperature profiles for a power law fluid with $n=0.50$ flowing in a slit whose walls are maintained at a constant temperature ($N_{Br}=1$).

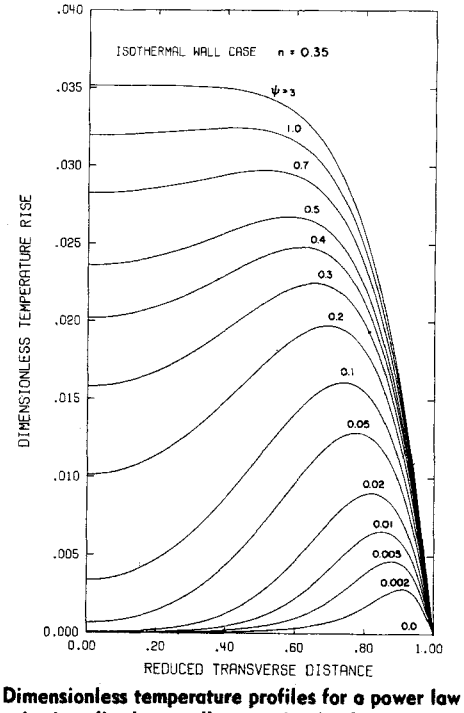

Figure 6. Dimensionless temperature profiles for a power law fluid with $n=0.35$ flowing in a slit whose walls are maintained at a constant temperature ($N_{Br}=1$).

C_n, obtained from numerical integration of Equations (31) and (32), are also given in Tables 1 and 2. The resultant eigenfunctions for the Newtonian and this power law fluid are tabulated in Tables 3 and 4, respectively.

Using the expressions Equations (29) and (30) for the temperature distribution and the information contained in Tables 1 to 4, we computed the temperature profiles for the isothermal and adiabatic wall cases as a function of the reduced axial distance ψ. In the calculation of all these profiles, we have used $N_{Br} = 1$. To obtain the temperature profile for any other Brinkman number, one merely multiplies the above results by the desired Brinkman number. Figures 3 to 7 show the development of the temperature profile in the Newtonian and power law fluids for slit walls which are isothermal. For these cases of isothermal walls, the temperature profile attains a fully developed condition near a reduced axial distance of 3. The adiabatic wall temperature profiles for the Newtonian and power law fluids are given in Figures 8 to 12. Adiabatic results appear in a graphical form similar to the isothermal ones, but a major difference is due to the fact that temperatures continue to rise with increasing slit length. The last profile shown in each of these figures for the adiabatic results represents the value of the reduced axial distance where the profile is fully developed with respect to the transverse variable η. For values ψ beyond the last one given in the figure, the temperature profile can be obtained by adding a factor of $\Delta\psi/N$ to the last given profile, where $\Delta\psi$ is the distance

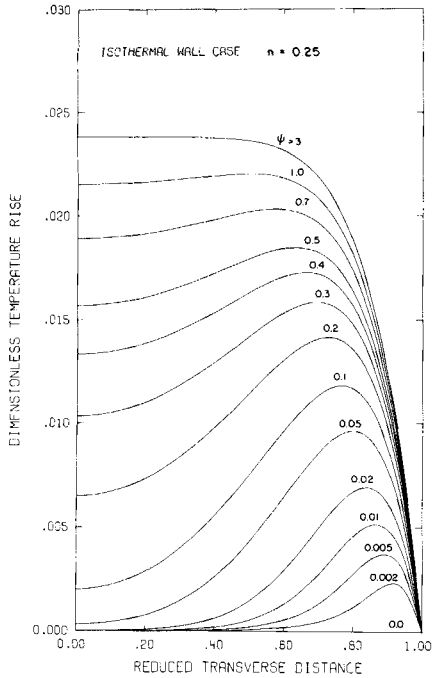

Figure 7. Dimensionless temperature profiles for a power law fluid with $n=0.25$ flowing in a slit whose walls are maintained at a constant temperature ($N_{Br}=1$).

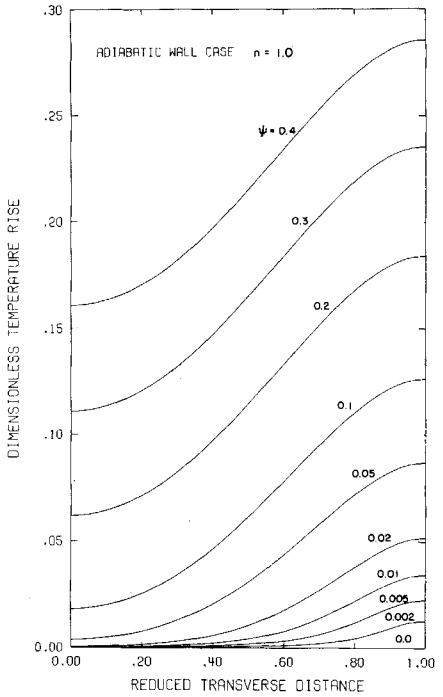

Figure 8. Dimensionless temperature profiles for a Newtonian fluid flowing in a slit with adiabatic walls ($N_{Br}=1$).

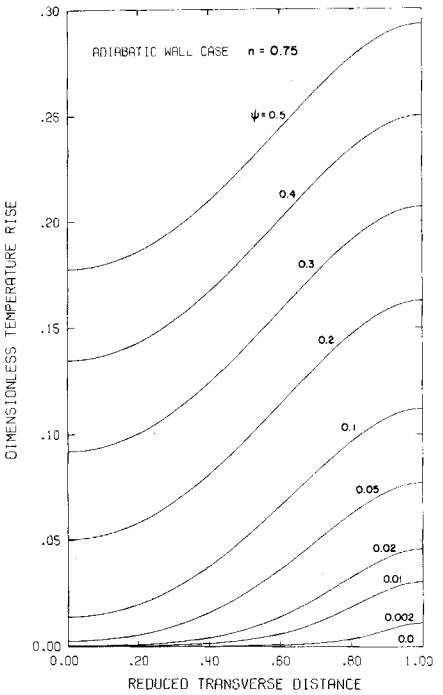

Figure 9. Dimensionless temperature profiles for a power law fluid with $n=0.75$ flowing in a slit with adiabatic walls ($N_{Br}=1$).

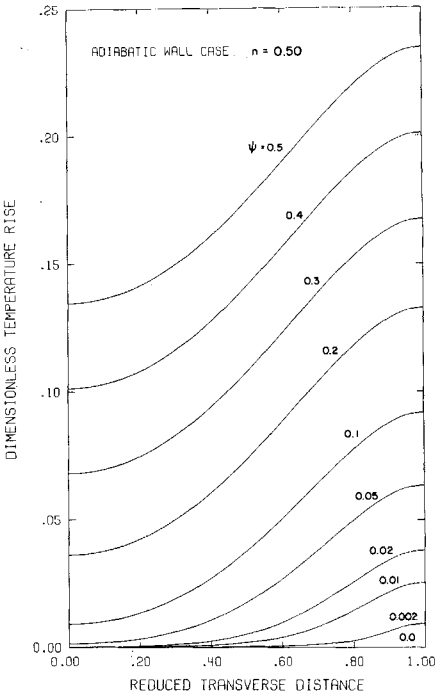

Figure 10. Dimensionless temperature profiles for a power law fluid with $n=0.50$ flowing in a slit with adiabatic walls ($N_{Br}=1$).

beyond the last given profile. The bulk temperature rises calculated via numerical integration of Equation (34) are given in Figures 13 and 14 for the isothermal and adiabatic wall cases, respectively. The maximum rises are conveniently extracted from the profiles given in Figures 3 to 12. We can see for the isothermal case from Figures 3 to 7 that the maximum migrates from the wall to the slit center line, whereas for the adiabatic case the maximum always occurs at the wall.

From the profiles given in Figures 3 to 12, it appears that Newtonian fluids at the same Brinkman number produce higher temperature rises than do their power law counterparts. However, such a direct comparison cannot be made between the Newtonian and non-Newtonian fluids because fixing the n value sets only one of the two parameters of power law model. Therefore, calculations of temperature rise must be done for each specific model.

Of the previous investigators of viscous heating of non-Newtonian fluids in slit flow, only Winter (1975) provided results for the developing temperature field and then just for one value $n = 0.4$. The possibility of using these profiles for estimating the temperature fields in extruder dies is suggested, but the single reported value of n greatly hampers his cause. Vlachopoulos and Keung (1972) presented graphically for $n = 0.5$ the bulk temperature rise and local Nusselt number as a function of the dimensionless distance ψ between 0.02 and 1.0 for a limited range of Brinkman numbers between $\pm$ 1.0. The nega-

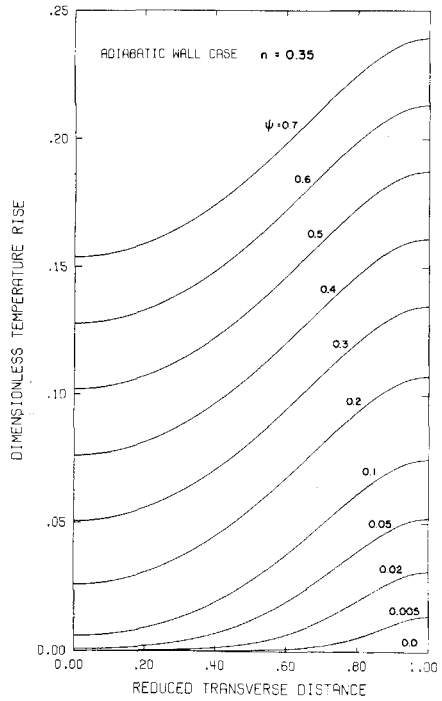

Figure 11. Dimensionless temperature profiles for a power law fluid with $n=0.35$ flowing in a slit with adiabatic walls ($N_{Br}=1$).

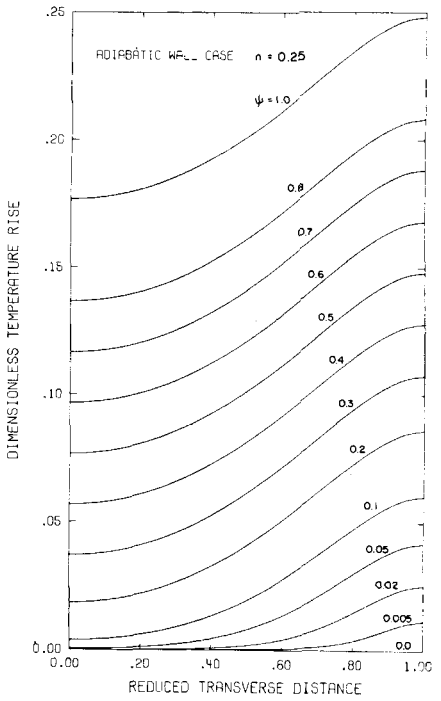

Figure 12. Dimensionless temperature profiles for a power law fluid with $n=0.25$ flowing in a slit with adiabatic walls ($N_{Br}=1$).

tive Brinkman numbers arise when the fluid enters at a lower temperature than the wall. Cox and Macosko (1974) presented correlated experimental data of the surface temperature rise, a result which is not useful in the prediction of the temperature rise across the slit. All of the above-mentioned treatments are strictly numerical in nature and suffer from the fact their solution does not span a wide enough range of flow conditions, for example, flow indexes and Brinkman numbers. Since our results are analytical, they can readily cover the wide range of flow indexes normally encountered for any Brinkman number (extent of viscous heating) and thus are most useful for deciding if viscous heating is appreciable during rheological property determination.

ACCURACY OF THE RESULTS

The differential equation subjected to the isothermal wall boundary conditions is an equation similar to the Graetz equation. Brown (1960) has presented a very accurate solution of the Graetz and associated problems for heat transfer in a Newtonian fluid but without viscous heating. His solution gives the first ten eigenvalues and first six eigenfunctions for values of η between 0 and 1 at increments of 0.05. Therefore, to test the accuracy of our numerical scheme, the results of our calculation of the Newtonian heat transfer problem were compared to Brown's calculations.

A comparison of the eigenfunctions of Brown's rounded to five places to ours presented in Table 3 shows a maximum deviation of $+0.00021$ occurring at $\eta = 0.1$ for F_5. The rest are within ± 0.0001 of the values given in Brown's paper. Our first six eigenvalues are for the Newtonian fluid case are presented in Table 1 to six significant figures. Our eigenvalues compare favorably to those reported by Brown, with the difference in the sixth eigenvalue being -0.005%. The reader should note that the coefficients listed in Table 1 are for the heat transfer problem with viscous heating. We have not presented the complete solution to the heat transfer problem without viscous heating. The solution involves evaluating the coefficients in Equation (31) subject to the proper condition posed at the slit entrance. The calculation of the eigenvalues and eigenfunctions are valid in both cases, since the solutions of the resultant homogeneous differential equations are identical when the appropriate nondimensionalization is performed.

As previously mentioned, Suckow et al. (1971) solved the heat transfer problem without viscous heating for both a Newtonian and non-Newtonian fluid (power law fluid with $n = 0.5$). Suckow's solution used only the first two terms in the series expansion. Table 5 and 6 show the two eigenvalues calculated by Suckow et al. and the present authors. A comparison of Suckow's et al. two eigenvalues with the first two presented by Brown clearly demonstrates that the solution of Suckow et al. is in error; for example, the second eigenvalue of Suckow et al. is 6.45%

TABLE 5. EIGENVALUES FOR THE HEAT TRANSFER OF A NEWTONIAN FLUID IN A SLIT WITH ISOTHERMAL WALLS

	λ_1	λ_2	λ_3	λ_4	λ_5	λ_6
Suckow et al. (1971)	2.834	34.220				
Brown (1960)	2.82776	32.1473	93.4749	186.805	312.136	469.468
Ybarra and Eckert	2.82776	32.1472	93.4740	186.801	312.126	469.444

TABLE 6. EIGENVALUES FOR THE HEAT TRANSFER OF A POWER LAW FLUID ($n = 0.5$) IN A SLIT WITH ISOTHERMAL WALLS

	λ_1	λ_2	λ_3	λ_4	λ_5	λ_6
Suckow et al. (1971)	2.787	31.934				
Ybarra and Eckert	2.64659	28.1319	81.5665	162.898	272.117	409.222

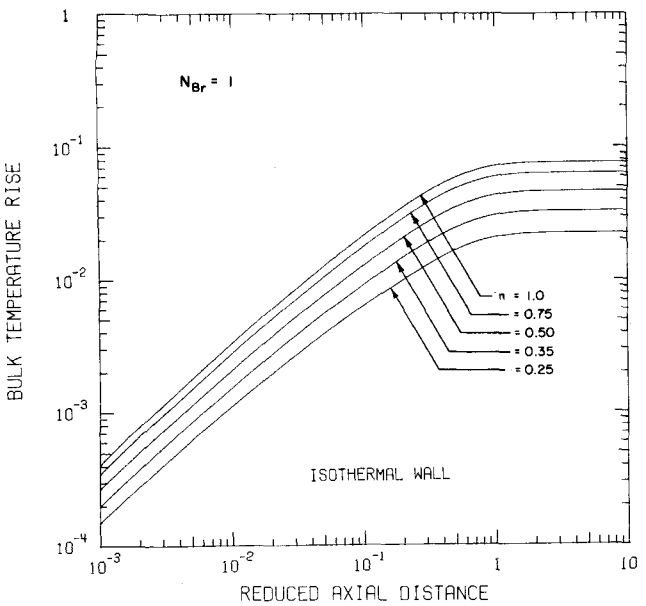

Figure 13. Bulk temperature rises for various power law fluids flowing in an isothermal slit (N_{Br}=1).

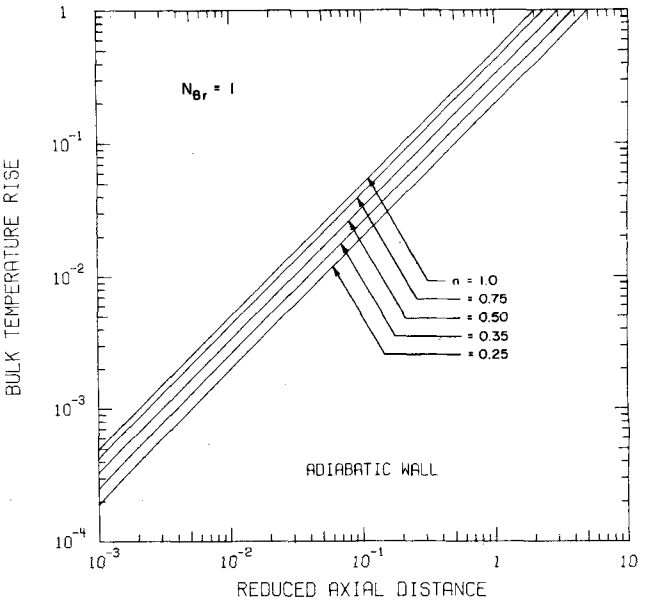

Figure 14. Bulk temperature rises for various power law fluids flowing in an adiabatic slit (N_{Br}=1).

higher than Brown's. This error will cause the bulk temperature rise calculation to be high in the range of low ψ, which is exactly what Vlachopoulos and Keung (1972) found in their numerical solution to this problem. Since our solution of the homogeneous problem is in accord with Brown's, and the particular solution is an analytical one in closed from, we conclude our results are accurate.

EXAMPLE OF CALCULATING TEMPERATURE RISES

For the purpose of demonstrating how the solution is used, we shall consider the following example taken from the experimental work of Cox and Macosko (1974): Molten ABS at 473°K flows through a slit of depth $2H = 4.57 \times 10^{-4}$m, width $W = 4.0 \times 10^{-2}$m, and length $L = 2.68 \times 10^{-2}$m. We will determine the maximum temperature and average temperature rise in the slit when the apparent shear rate is 2 000 s^{-1}. The following physical properties for ABS at the above conditions are:

$$k = 0.279 \text{ W/m °K}$$

$$\hat{C}_p = 2.26 \times 10^3 \text{ j/kg °K}$$

$$\rho = 979 \text{ kg/m}^3$$

$$n = 0.35$$

$$K = 2.36 \times 10^4 \text{ s}^{0.35} \text{ N/m}^2$$

The wall shear stress can be calculated from the relationship

$$\tau_w = K'\dot{\gamma}_a^n = (2.36 \times 10^4)(2000)^{0.35} = 3.37 \times 10^5 \text{ N/m}^2 \quad (48)$$

By combining Equations (12) and (14), we can write the reduced axial distance as

$$\psi = \frac{kx_1 N}{\rho \hat{C}_p H^3}\left(\frac{K}{\tau_w}\right)^{1/n} \quad (49)$$

The maximum temperature rise in the slit will occur at the exit. The dimensionless axial distance ψ at the exit is

$$\psi = \frac{(0.279)(2.68 \times 10^{-2})(1.35/0.35)(2.36 \times 10^4)^{1/0.35}}{(979)(2.26 \times 10^3)(2.285 \times 10^{-4})^3(3.37 \times 10^5)^{1/0.35}} = 0.55$$

Likewise, the Brinkman number can be expressed in terms of τ_w to give

$$N_{Br} = \frac{H^2}{kT_w}\left(\frac{\tau_w}{K}\right)^{1/n}\tau_w \quad (50)$$

$$N_{Br} = \frac{(2.285 \times 10^{-4})^2(3.37 \times 10^5)^{1.35/0.35}}{(0.279)(473)(2.36 \times 10^4)^{1/0.35}} = 0.266$$

For the reduced axial distance of 0.55, the maximum dimensionless rises are obtained by the interpolation of Figures 6 and 11. The corresponding average rises are found from Figures 13 and 14, and these values are presented in Table 7.

TABLE 7. DIMENSIONLESS TEMPERATURE RISES

	θ_{max}	θ_{av}
Isothermal wall	0.028	0.025
Adiabatic wall	0.200	0.147

To obtain the actual temperature rise in the slit, we multiply the dimensionless temperature rises, which are based upon a Brinkman number of unity, by the Brinkman number of the flow situation 0.266. For the maximum temperature rise in a slit whose walls are operating isothermally, we can calculate the temperature rise:

$$(T-T_w)_{max} = N_{Br}\, T_w\, \theta_{max}\Big|_{N_{Br}=1} \quad (51)$$

$$(T-T_w)_{max} = (0.266)(473)(0.028) = 4°\text{K}$$

The results for the maximum and average rises are given in Table 8.

TABLE 8. TEMPERATURE RISE RESULTS (°K)

	$(T-T_0)_{max}$	$(T-T_0)_{av}$
Isothermal wall	4	3
Adiabatic wall	25	18

Thus, even with perfect cooling, that is, the slit wall is a precisely the temperature of the entering polymer, the fluid experiences a few degrees temperature rise. Properties determined as if isothermality were maintained would, therefore, be subject to an error beyond the desired degree of accuracy. The property reported at the average instead of the inlet temperature might prove satisfactory. However, if less efficient cooling were applied to the slit, the maximum and the average temperature rises would approach the adiabatic values in Table 8. With the large resultant temperature rises, use of a simple temperature correction based upon the average would be inadequate.

It has been shown that polymer melts subjected to moderate shear rate generate sufficient heat to cause errors in stress property measurement, even when the walls are maintained at constant temperature. We will now compare polymer solutions with melts in a semiquantitative manner to contrast the effects involved. For both polymer melts and solutions subjected to the same shear rate, typical values of the ratio $k/\rho\hat{C}_p$ and thermal conductivity are 10^{-7} m²/s and 10^{-1} W/m°K, respectively (Middleman, 1968). From experimental data given in Bird et al. (1977) for solutions and melts at high shear rates, the ratio τ_w/K for melts and solutions are approximately the same, whereas the wall shear stress for a polymer melt may be 10^3 times greater. With the ratios $k/\rho\hat{C}_p$ and τ_w/K and the thermal conductivity the same in the melts and solutions, the reduced axial distance is also constant. However, the Brinkman number is proportional to τ_w, so this number for the melt would be a factor of τ_w greater than for the solution. Since the temperature rise is proportional to the Brinkman number for a polymer solution flowing at the same shear rate as the polymer melt in our example, we would estimate the temperature rise in the slit to be negligible, less than 0.1°K.

DETERMINING RHEOLOGICAL PROPERTIES WITH A MINIMUM TEMPERATURE RISE

When the measurement of a rheological property is made, it is of paramount importance to keep the amount of viscous heating during the experiment to a minimum. From the previous example, it is obvious that the temperature rise can be greatly reduced by maintaining the slit walls at a constant temperature. Here, we wish to explore how the extent of viscous heating in a slit with isothermal walls can be diminished by varying the slit geometry. From Equation (51) it can be seen that reducing the Brinkman number and the dimensionless temperature rise decreases the actual temperature rise. However, this situation is complicated by the fact that variables which enter the Brinkman number also appear in the dimensionless distance ψ. This interaction between the Brinkman number and the reduced axial distance on the temperature rise will be explored below.

We wish to minimize viscous heating for a fluid deforming at a given wall shear rate. One further requirement is that ratio L/H remain constant, since we assume that we know a priori the value of this ratio required to realize a viscometric flow regime. If we now refer back to Equations (49) and (50), we find that by holding the above mentioned experimental conditions constant

$$\psi(H) \propto H^2 \tag{52}$$

$$N_{Br}(H) \propto H^2 \tag{53}$$

If the slit thickness is halved, the Brinkman number decreases fourfold, whereas the reduced axial distance increases fourfold. The dimensionless temperature rise is a more complicated function of ψ. Figure 13 shows for small values of ψ a fourfold increase produces a change in the dimensionless temperature rise which is slightly less than fourfold, while for large values of ψ the corresponding change is zero. Thus, the dimensionless temperature rise θ always increases with H by a smaller factor than does ψ:

$$\theta(\psi) \propto H^n \text{ where } 0 \geq n > -2 \text{ for } \infty > \psi > 0 \tag{54}$$

Substituting in Equation (51), the above expressions for N_{Br} and θ, we find

$$(T - T_w) \propto H^n \text{ where } 2 \geq n > 0 \text{ for } \infty > L > 0 \tag{55}$$

Equation (55) shows the overall effect of increasing H is an increase in the temperature rise.

To demonstrate this point, we shall halve the slit height and length in the above example and calculate the average temperature rise. For the smaller height channel, the reduced axial distance increases to 2.2, the Brinkman number decreases to 0.067 and from Figure 13 the average dimensionless temperature rise is found to be 0.035. Thus, to calculate the temperature rise, Equation (51) gives

$$(T - T_0)_{avg}(0.067)(473)(0.035) = 1°K$$

Comparing this result to the value of 3°K given in Table 8 for the average temperature rise in an isothermal wall slit, we see that a net reduction in the temperature rise due to viscous heating has been realized.

We conclude that in order to minimize the effect of viscous heating during the measurement of rheological properties, one should use as thin a slit as possible, the lower limit on the slit thickness being set by the accuracy to which channels and pressure sensing devices can be constructed to form a completely uniform slit.

NOTATION

A = matrix defined by the left-hand side of Equation (47)
B = matrix defined by the right-hand side of Equation (47)
$\hat{C}_p$ = heat capacity at constant pressure per unit mass, j/kg°K
C_n = constants in Equations (29) and (30)
f = variable coefficient of x in Equation (38)
$\underline{f}$ = eigenvector representing the eigenfunction at the specified grid points
F = separation function in η only
G = separation function in ψ only
h = step size of finite difference
H = slit half width, m
k = thermal conductivity, W/m°K
K = flow consistency of power law fluid, $N \cdot s^n/m^2$
M = number of intervals in the finite difference
n = flow index
N = $(n + 1)/n$
T = temperature, °K
v = velocity, m/s
x = cartesian coordinate
x = independent variable in Equation (38)
y = function of x in Equation (38)

Greek Letters

$\dot{\gamma}$ = shear rate, s^{-1}
η = viscosity function defined by Equation (3)
η = reduced transverse distance defined by Equation (13)
θ = reduced temperature defined by Equations (15) and (16)
λ = eigenvalue
Ξ = function in Equations (21) and (23)
ρ = fluid density, kg/m³
τ = shear stress, N/m²
ϕ = function in Equations (21) and (23)
χ = function in Equation (23)
ψ = reduced axial distance defined by Equation (14)

Dimensionless Groups

N_{Re} = Reynolds number
N_{Pr} = Prandtl number
N_{Br} = Brinkman number for power law fluid defined by Equation (20)
N_{Pe} = Peclet number

Subscripts

av = mixing-cup average
max = maximum
0 = initial
w = wall
1 = direction of flow
2 = direction transverse to the flow

LITERATURE CITED

Bird, R. B., "Viscous Heat Effects in Extrusion of Molten Plastics," *SPE J.*, **11**, 35 (1955).

———., W. E. Stewart and E. N. Lightfoot, *Transport Phenomena*, Wiley, New York (1960).

Bird, R. B., R. C. Armstrong and O. Hassager, *Dynamics of Polymeric Liquids*, Vol. 1, Fluid Mechanics," Wiley, New York (1977).

Brinkman, H. C., "Heat Effects in Capillary Flow," *Appl. Sci. Res.*, **A2**, 120 (1951).

Brown, G. M., "Heat or Mass Transfer in a Fluid in Laminar Flow in a Circular or Flat Conduit," *AIChE J.*, **6**, 179 (1960).

Churchill, R. V., *Fourier Series and Boundary Valve Problems*, 2 ed., McGraw-Hill, New York (1963).

Cox, H. W., and C. W. Macosko, "Viscous Dissipation in Die Flows," *AIChE J.*, **20**, 785 (1974).

Dang, V. D., "Low Peclet Number Heat Transfer for Power Law Non-Newtonian Fluid with Heat Generation," *J. Appl. Polymer Sci.*, **23**, 3077 (1979).

Galili, N., R. Takserman-Krozer and Z. Rigbi, "Heat and Pressure Effect in Viscous Flow Through a Pipe, I. General Formulation and Basic Solution," *Rheol. Acta*, **14**, 550 (1975*a*).

———., "Heat and Pressure Effect in Viscous Flow Through a Pipe, II. Analytical Solution for Non-Newtonian Flow," *ibid.*, 816 (1975*b*).

Gavis, J., and R. L. Laurence, "Viscous Heating of a Power-Law Liquid in Plane Flow," *Ind. Eng. Chem. Fundamentals*, **7**, 525 (1968).

Gee, R. E., and J. B. Lyon, "Nonisothermal Flow of Viscous Non-Newtonian Liquids," *Ind. Eng. Chem.*, **49**, 956 (1956).

Hieber, C. A., "Thermal Effects in the Capillary Rheometer," *Rheol. Acta*, **16**, 553 (1977).

Hildebrand, F. B., *Introduction to Numerical Analysis*, McGraw-Hill, New York (1974).

Kwant, P. B., and Th. N. M. Van Ravenstein, "Non-isothermal Laminar Channel Flow," *Chem. Eng. Sci.*, **28**, 1935 (1973).

Middleman, S., *The Flow of High Polymers*, Interscience, New York (1968).

Novotny, E. J., and R. E. Eckert, "Direct Measurement of Hole Error for Viscoelastic Fluids in Flow Between Infinite Parallel Plates," *Trans. Soc. Rheol.*, **17**, 222 (1973).

———., "Rheological Properties of Viscoelastic Fluids from Continuous Flow Through a Channel Approximating Infinite Parallel Plates," *ibid.*, **18**, 1 (1974).

Seifert, A., "Wärmeübergang bei der Strömung von Prandtl-Eyring-Flüssigkeiten durch ebene Spalte. Mit Berücks. d. Dissipation u. umsymmetr. therm. Randbediggn." Doctoral thesis, Technische Universität, Berlin (1969).

Suckow, W. H., P. Hrycak and R. G. Griskey, "Heat Transfer to Polymer Solutions and Melts Flowing Between Parallel Plates," *Polymer Eng. Sci.*, **11**, 401 (1971).

Sukanek, P. C., "Poiseuille Flow of a Power-Law Fluid with Viscous Heating," *Chem. Eng. Sci.*, **26**, 1775 (1971).

Tien, C., "The Extension of Couette Flow Solution to the Non-Newtonian Fluid," *Can. J. Chem. Eng.*, **39**, 45 (1961).

———., "Laminar Heat Transfer of Power-Law Non-Newtonian Fluid—The Extension of Graetz-Nusselt Problem," *ibid.*, **40**, 130 (1962).

Toor, H. L., "The Energy Equation for Viscous Flow: Effect of Expansion on Temperature Profiles," *Ind. Eng. Chem.*, **48**, 922 (1956).

———., "Heat Generation and Conduction in the Flow of a Viscous Compressible Liquid," *Trans. Soc. Rheol.*, **1**, 177 (1957).

Turian, R. M., "Viscous Heating in the Cone and Plate Viscometer, III, Non-Newtonian Fluids with Temperature Dependent Viscosity and Thermal Conductivity," *Chem. Eng. Sci.*, **20**, 771 (1965).

Vlachopoulos, J., and C. K. J. Keung, "Heat Transfer to a Power-Law Fluid Flowing Between Parallel Plates," *AIChE J.*, **18**, 1272 (1972).

Winter, H. H., "Temperature Fields in Extruder Dies with Circular, Annular, or Slit Cross-Section," *Polymer Eng. Sci.*, **15**, 84 (1975).

———., "Viscous Dissipation in Shear Flows of Molten Polymers," *Adv. Heat Transfer*, **13**, 205 (1977).

Wohl, M. H., "Designing for Non-Newtonian Fluids, Part 5, Dynamics of Flow Between Parallel Plates and in Noncircular Ducts," *Chem. Eng.*, **75**, 183 (May 6, 1968).

Manuscript received August 29, 1979; revision received January 17, and accepted January 25, 1980.

Heat Transfer from Two-Phase Boundary Layers on Isothermal Cylinder: Influence of Drop Trajectory

The influence of drop trajectories on boundary layer structure and heat transfer coefficient is determined for a binary spray flow over the upstream surface of an isothermal cylinder. Governing equations are solved for drop trajectories upstream of the cylinder, the laminar liquid boundary layer adjacent to the cylinder surface, and the outer laminar vapor boundary layer. Velocity, temperature, and mass concentration profiles throughout the double boundary layers are shown to depend on flow parameters involving drop size and velocity. The critical conditions for which the liquid film dries out are identified for a range of drop size and velocity, defining the transition from the liquid film to the dry wall flow regime. Theoretical results for heat transfer are shown to correlate existing experimental data.

CHRISTOPHER C. LU

and

JOHN W. HEYT

Department of Chemical Engineering
The University of Dayton
Dayton, Ohio 45469

SCOPE

The increase in surface heat transfer resulting from the addition of liquid drops to a gas stream may contribute a significant reduction in size and operating cost of a heat exchanger. The application can also be used for the emergency cooling system in a nuclear reactor where liquid drops can be sprayed directly across a heating surface. The objective of this study is to identify the effect of drop trajectory on the boundary layer structure and on the local heat transfer coefficient for a binary spray flow perpendicular to an isothermal cylinder. Drops of a single-component liquid are dispersed uniformly throughout the binary gas, which is composed of the vapor of the liquid drops and a noncondensable component. Gas and liquid flows are retarded near the stationary cylinder surface, forming a boundary layer. Drops which impinge on the cylinder surface form a liquid film which enhances the wall heat transfer.

John W. Heyt is with General Electric Corporation, South Portland, Maine 04104.

0001-1541-80-3731-0762-$00.95.